© 2022. Published by The Company of Biologists Ltd | Development (2022) 149, dev199667. doi:10.1242/dev.199667

TECHNIQUES AND RESOURCES

RESEARCH REPORT

Long-term imaging of living adult zebrafish

Daniel Castranova, Bakary Samasa, Marina Venero Galanternik, Aniket V. Gore, Allison E. Goldstein, Jong S. Park and Brant M. Weinstein*

ABSTRACT

The zebrafish has become a widely used animal model due, in large part, to its accessibility to and usefulness for high-resolution optical imaging. Although zebrafish research has historically focused mostly on early development, in recent years the fish has increasingly been used to study regeneration, cancer metastasis, behavior and other processes taking place in juvenile and adult animals. However, imaging of live adult zebrafish is extremely challenging, with survival of adult fish limited to a few tens of minutes using standard imaging methods developed for zebrafish embryos and larvae. Here, we describe a new method for imaging intubated adult zebrafish using a specially designed 3D printed chamber for long-term imaging of adult zebrafish on inverted microscope systems. We demonstrate the utility of this new system by nearly day-long observation of neutrophil recruitment to a wound area in living double-transgenic adult *casper* zebrafish with fluorescently labeled neutrophils and lymphatic vessels, as well as intubating and imaging the same fish repeatedly. We also show that Mexican cavefish can be intubated and imaged in the same way, demonstrating this method can be used for long-term imaging of adult animals from diverse aquatic species.

KEY WORDS: Zebrafish, Adult, Imaging, Intubation, Neutrophil, Lymphatic

INTRODUCTION

High-resolution *in vivo* imaging of developmental, regenerative or other processes in vertebrate animals is extremely challenging after embryonic or early larval stages, involving sophisticated technical methods to ensure the health and survival of heavily anesthetized, rigidly immobilized juvenile or adult animals. Although a variety of methods have been developed for long-term anesthetization and imaging of terrestrial vertebrates, including humans and research models such as mice, rats and cats, there has been limited application of these types of method to aquatic vertebrates, despite their wide use as powerful research model organisms. The zebrafish is the most widely used aquatic vertebrate model organism. They are small, allowing many fish to be housed in a relatively small space, and they produce large numbers of externally developing offspring at frequent intervals for genetic and experimental studies. Mutagenesis screens in fish have identified thousands of mutations with defects in embryonic development (Driever et al., 1996; Mullins et al., 1994), the characterization of which has led to innumerable important new insights (Patton and Zon, 2001), and reverse genetic tools such as morpholinos (Nasevicius and Ekker, 2000) and CRISPR (Hwang et al., 2013) have been used to target specific genes of interest. The optical clarity of zebrafish embryos and early larvae facilitates very high-resolution optical imaging of all developing organs and tissues, including those deep within the animal. Thousands of transgenic lines have been developed that permit spatial and temporal control of gene expression (Scheer and Campos-Ortega, 1999; Wyart et al., 2009) or use fluorescent reporters to 'mark' and permit study of a wide variety of different organs and tissues, including blood and lymphatic vessels (Jung et al., 2017; Lawson and Weinstein, 2002; Yaniv et al., 2006), the nervous system (Wyart and Del Bene, 2011), the liver and pancreas (Ober et al., 2003), and many others.

Although the historical focus of zebrafish research has been on embryonic and larval development, there has recently been increasing interest in using zebrafish to study processes such as disease and tissue regeneration in adults. Studies in adult zebrafish have led to novel insights into cancer metastasis (Kaufman et al., 2016) with potential for new treatments (Frantz and Ceol, 2020). Human tumors transplanted into zebrafish are being used as a platform for developing precision cancer therapies (Fazio et al., 2020; Yan et al., 2019). Zebrafish have also been used to model obesity and diabetes, with recent work showing that the pathophysiological pathways are conserved between mammals and zebrafish (Oka et al., 2010). The ability of zebrafish to regenerate complex tissues, including the fins (Johnson and Weston, 1995) and heart (Poss et al., 2002), makes them a superb model for understanding mechanisms that control tissue regeneration. There are also many tissues and processes that do not exist during early embryonic and larval development, such as the newly described intracranial lymphatic vascular network (Castranova et al., 2021), a fully functional adult immune system and adult regeneration processes that can only be imaged and studied in juveniles and adults.

Although there has been significant progress in the use of adult zebrafish as research model, microscopic imaging of adult zebrafish and other adult aquatic vertebrates remains extremely challenging. Even if they are kept submerged, anesthetized adult zebrafish can only be imaged for a few tens of minutes before the animal dies, generally from lack of adequate oxygenation. In terrestrial models, longer-term live imaging generally involves anesthesia with intubation to ensure that the animal remains oxygenated and viable during imaging. A previous report from Xu et al. described a method for intubating and holding adult zebrafish for live imaging on an upright microscope (Xu et al., 2015), which was further adapted by Cox et al. (2018) to look at osteoblasts in regenerating scales. Here, we describe a redesigned method designed for inverted microscopes that includes a variety of powerful new features, including easily replicated 3D printed imaging chambers, multiple levels of newly designed safety features to prevent water overflow onto microscope optics, tight control of temperature and pulse dampening of inflow water to eliminate motion of the imaged sample. We also provide easy-to-use instructions for replicating our

Division of Developmental Biology, Eunice Kennedy Shriver National Institute of Child Health and Human Development, NIH, Bethesda, MD 20892, USA.

*Author for correspondence (weinsteb@mail.nih.gov)

B.M.W., 0000-0003-4136-4962

Handling Editor: Kenneth Poss
Received 30 March 2021; Accepted 30 November 2021

Development (2022) 149, dev199667. doi:10.1242/dev.199667

methods, including downloadable, easily modifiable CAD designs for the 3D (three dimensional) printed imaging chambers, and detailed user guides and instructions. We demonstrate the power and utility of our system by carrying out long-term imaging of neutrophil recruitment to wounds in adult zebrafish with transgenically labeled neutrophils and lymphatic vessels, including repeated intubation and imaging of the same fish over the course of a week. We also show that our intubation system can be used for aquatic species besides zebrafish by intubating and imaging Mexican cavefish (*Astyanax mexicanus* – Pachon), demonstrating the broad usefulness and applicability of our methods for high-resolution long-term *in vivo* imaging of aquatic vertebrates.

RESULTS

Previously, we reported methods for short-term and long-term imaging of developing zebrafish embryos and larvae (Kamei and Weinstein, 2005), but these methods are not suitable for imaging adult zebrafish. We have now designed a modified, improved chamber and associated 'rig' for long-term time-lapse imaging of live adult zebrafish (Fig. 1). The required equipment is compact and can easily be incorporated into any inverted microscopy workspace with minimal disruption (Fig. 1A), and is easy to assemble (Fig. S1). Intubation provides a continuous flow of oxygenated water through the gills of the fish (Fig. 1B-D). The apparatus includes a custom-designed 3D-printed plastic chamber (Fig. 1E,F, https://3dprint.nih.gov/discover/3dpx-016689) that incorporates a variety of useful features, including a digital thermometer monitoring water temperature (Fig. S2) and a single four-line peristaltic pump that provides the necessary force for water flow through the single inflow and dual larger outflow tubes (Fig. 1B), ensuring that inflow cannot exceed outflow (previous methods relied on use of multiple pumps, which could have differing flow rates or fail separately). We have also incorporated a pulse dampener (Fig. S3) that reduces movement caused by peristaltic pump pulsation. The design also incorporates multiple additional safety features to protect expensive microscope systems, including a water sensor (Fig. 1B,C, Fig. S4) connected to an emergency shut-off switch, in case both the redundant dual outflow tubes clog (Fig. 1B,C), and an emergency overflow tube (Fig. 1B) to shuttle excess liquid away and prevent chamber overflow if all else fails.

The schematic diagram in Fig. 2A provides an overview of the components of the intubation rig (Table S1) and how they are all assembled, while Fig. 2B,C shows details of the specific arrangement of components in and connected to the imaging chamber and Fig. S1 provides a detailed, step-by-step guide to assembly. The commercially available chambered coverglass (Lab Tek II Imaging Dish, Table S1) is secured to the printed intubation chamber using silicone grease, as shown in Fig. 2A and Fig. S1. As shown in these schematics, the various parts are easily assembled to form the

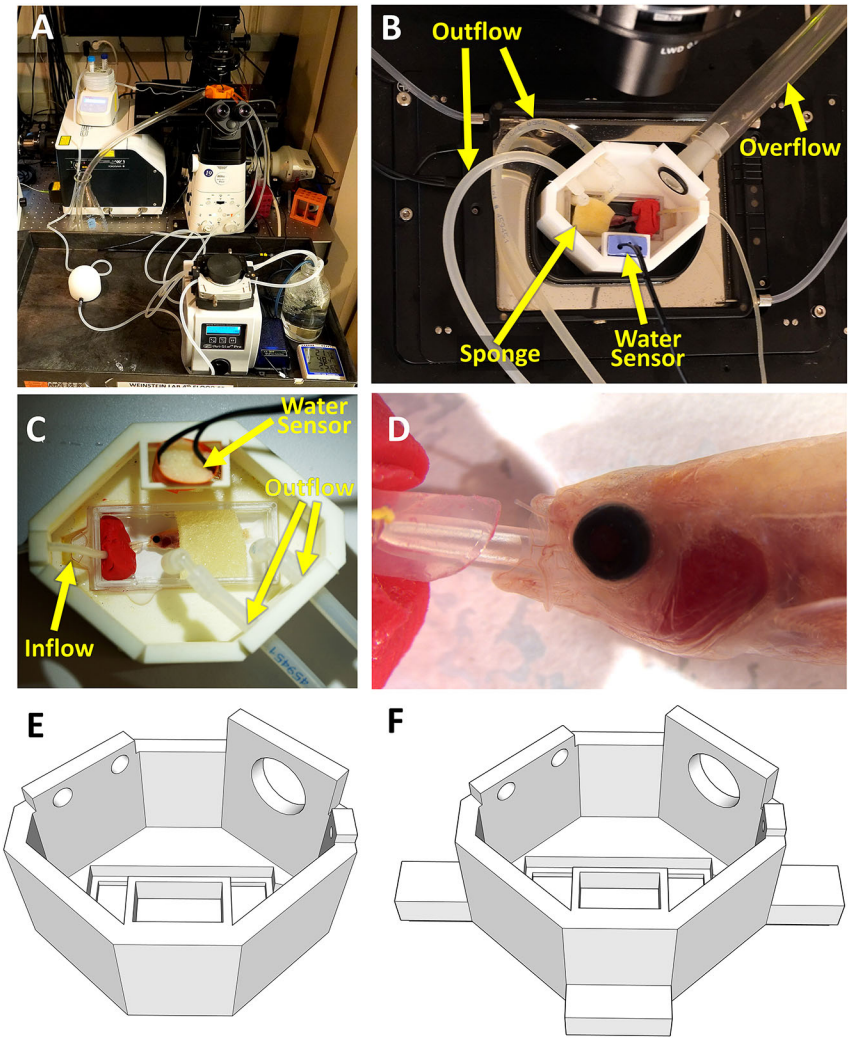

Fig. 1. Intubation of an adult fish on an inverted microscope. (A-D) Photographs of long-term imaging of an intubated adult zebrafish inside a custom 3D-printed chamber. (A) Overview photograph of an intubation rig set up on an inverted microscope. (B) Photograph of the intubation/imaging chamber set up on a microscope stage, showing inflow tube, dual outflow tubes, overflow tube, water sensor and sponge holding fish in place. (C) Close-up photograph of the chamber with an intubated fish, with inflow tube, dual outflow tubes and water sensor noted. (D) Higher magnification image of the intubated fish. (E,F) 3D renderings of intubation chambers designed to fit on (E) a Tokai Hit heated stage (model INUB-TIZB) or (F) in a 96-well plate holder on a Tokei Hit heated stage (model STZF-TIZWX-SET), or any other stage designed to hold 96-well plates.

Development (2022) 149, dev199667. doi:10.1242/dev.199667

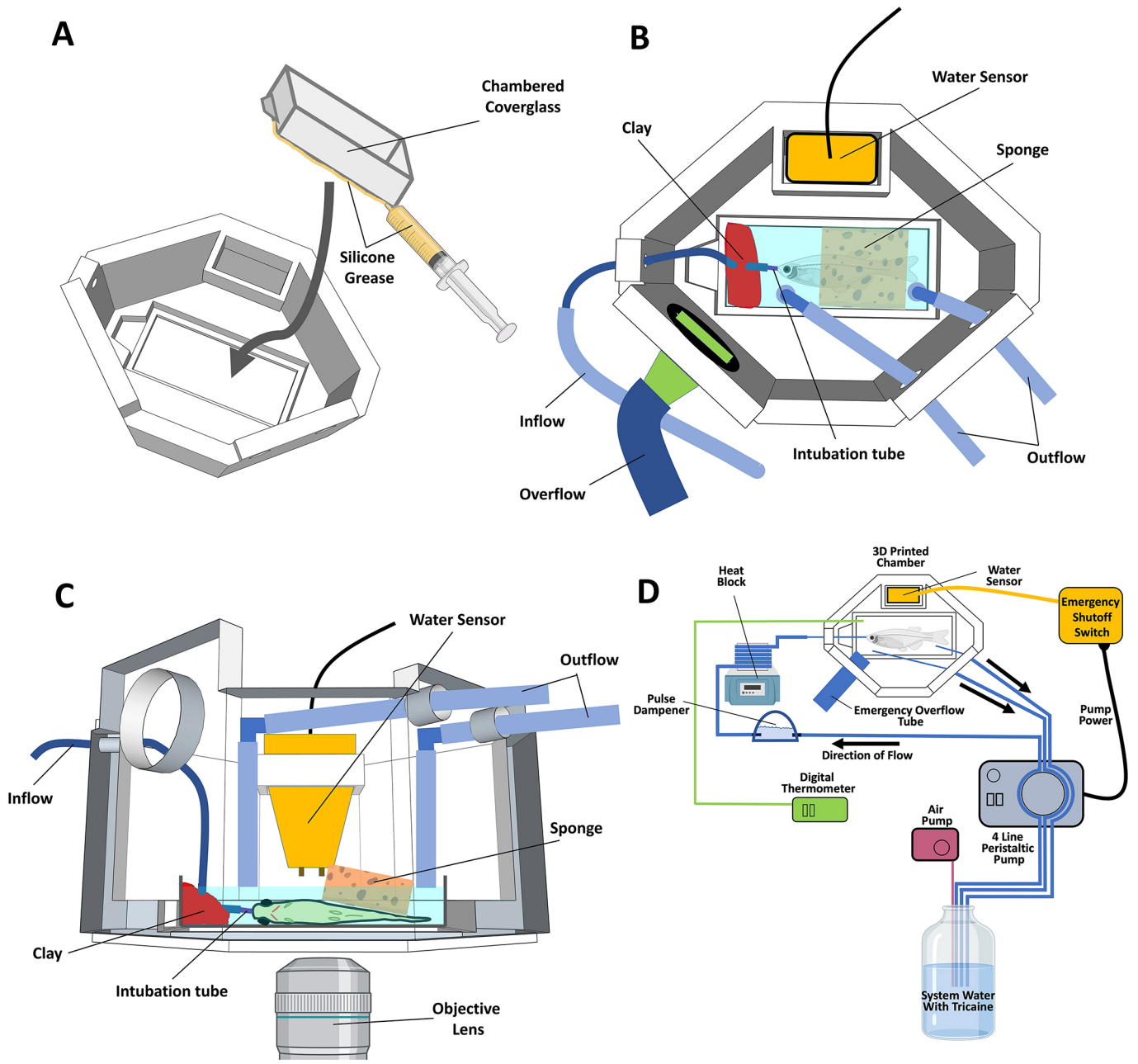

Fig. 2. Schematic diagrams of zebrafish intubation. (A) Schematic diagram showing attachment of a chambered coverglass into the 3D printed chamber, using silicone grease to provide a watertight seal. (B) Schematic diagram showing a top view of the intubation chamber. (C) Schematic diagram showing a side view of the intubation chamber. (D) Schematic diagram providing an overview of the arrangement and interconnection of components for fish intubation.

working unit without a great deal of technical knowledge (Fig. S1). We have provided two different versions of the chamber design: one designed to fit on our Tokei Hit heated stage (Fig. 1E); and one with four supports extending out from the base of the chamber body, which is designed to fit in a stage designed to hold 96-well plates (Fig. 1F). We chose the 96-well format because there are several microscope and stage companies that manufacture stages or inserts designed to fit the 96-well plate dimensions. We designed the chamber to fit on the heated stages we had on our microscopes, but because we use a heat block to warm the water before it enters the chamber, a heated stage is not required. Our design can be modified to fit other imaging systems using the computer aided design (CAD) software files deposited on the NIH 3D Print Exchange (https://3dprint.nih.gov/discover/3dpx-016689). The length of the four stage supports can be modified using Google SketchUp or other widely available CAD software to fit on many different microscope stages from a variety microscope manufacturers. The designs can be 3D printed using commercially available printing services (e.g. Xometry; Table S1). The rest of the intubation rig components, including the tubing, water sensor, pumps, water bath and thermometer are also commercially available (Table S1). This intubation rig is simple to replicate and cost-effective.

To demonstrate that anesthetized, intubated adult fish can survive for an extended time period in the chamber, we carried out a total of 26 runs on individual adult fish for at least 20 h, with a survival rate of 77% (20/26), a level similar to that observed in long-term time-lapse imaging experiments of comparable time length performed on zebrafish larvae (D.C., unpublished observations). We also

Development (2022) 149, dev199667. doi:10.1242/dev.199667

completed six shorter runs (3.5 h) and had 100% survival. To maximize survival, we have provided a 'tips and tricks' section at the end of our step-by-step assembly guide (Fig. S1).

To demonstrate the utility of this intubation set-up for high-resolution long-term confocal imaging of living adult zebrafish, we performed time-lapse imaging of neutrophil recruitment to a wound site in an adult zebrafish with transgenically labeled neutrophils and lymphatic vessels. We made a small wound on the side of an adult *Tg(lyz:DsRed2)*^{NZ50}*;Tg(mrc1a:eGFP)*^{y251} double transgenic *casper* mutant zebrafish. This line has red fluorescent neutrophils and green fluorescent lymphatic vessels (Fig. 3A), and the use of the pigment-free *casper* (*roy, nacre* double mutant; White et al., 2008) background provides improved tissue clarity for adult imaging. The endogenous blue autofluorescence of the scales allowed us to visualize where they were removed by wounding (Fig. 3B). Over the course of nearly day-long time-lapse imaging of living adult zebrafish, we were able to image neutrophils moving into and accumulating in the wound area (Fig. 3C-J, Movie 1). Interestingly, significantly increased neutrophil recruitment to the wound area does not begin until 2-3 h post-injury (Fig. 3D,H, Movie 1), which is much longer than an anesthetized zebrafish without intubation can survive, making intubation essential for studying this interesting process. By using a 20× long-working-distance objective, we were able to acquire high-magnification high-resolution images of highly active migratory neutrophils moving around and through lymphatic vessels close to the wound site (Fig. 3K-N, Movie 1).

We conducted additional experiments to examine whether overnight intubation of *Tg(lyz:DsRed2)*^{NZ50}*;Tg(mrc1a:eGFP)*^{y251} double transgenic *casper* mutant fish adult fish with or without overnight confocal imaging inhibits neutrophil recruitment after wounding, or whether intubation and imaging promotes neutrophil recruitment even in the absence of wounding (Fig. S5). We found no statistically significant difference in neutrophil recruitment to wounds overnight, regardless of whether or not the fish was intubated with or without continuous overnight imaging of the wounded area (Fig. S5C-E,H-K; compare conditions iii, iv and v). We also saw no statistically appreciable enhancement of neutrophil recruitment in unwounded animals promoted by intubation, in either the presence or absence of continuous overnight imaging (Fig. S5A,B,F,G,K; conditions i and ii). These results suggest the experimental methods we are using for intubation and for continuous overnight confocal imaging do not themselves have appreciable effects on neutrophil recruitment. However, we cannot exclude the possibility that prolonged intubation and imaging may cause other physiological changes within the fish, and appropriate controls must always be included, depending on the process being studied.

To determine whether our methods can be used for repeated anesthetization, intubation and imaging of the same fish on multiple days, we introduced a cutaneous wound on a *Tg(lyz:DsRed2)*^{NZ50}*;Tg(mrc1a:eGFP)*^{y251} double transgenic *casper* mutant fish as above then repeatedly intubated and carried out time-lapse confocal imaging on the same fish for 3.5 h at 0, 1, 2 and 7 days post-

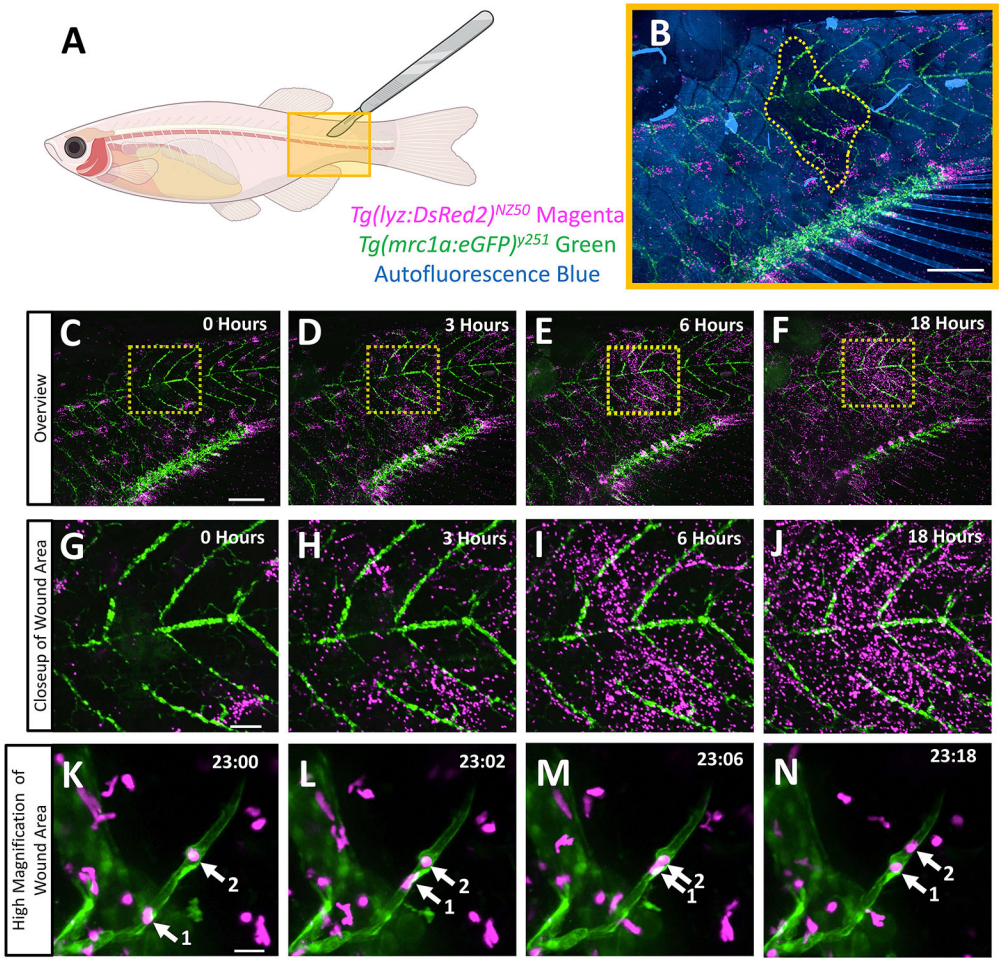

Fig. 3. Long-term time-lapse imaging of neutrophil recruitment to a scale-removal wound in an intubated adult zebrafish. (A) Schematic diagram of an adult *casper Tg(lyz:DsRed2)*^{NZ50}*; Tg(mrc1a:eGFP)*^{y251} double transgenic zebrafish. The approximate site of scale removal by abrasion with a scalpel is noted with a yellow box. (B) An overview image of the wound area (yellow box in A) at the start of time-lapse imaging. Fluorescent neutrophils (magenta), lymphatic vessels (green) and auto-fluorescent scales (blue) are visible. The yellow dashed line indicates the boundary of the site where auto-fluorescent blue scales were removed. (C-N) Maximum intensity projection still images from long-term time-lapse confocal imaging of the adult fish in B. (C-F) Overview confocal images of the trunk at 0 (C), 3 (D), 6 (E) and 18 (F) hours. (G-J) Close-up images of the boxed regions in C-F. (K,L) High-magnification images of neutrophils (magenta) actively migrating in and around lymphatic vessels (green) in the recovering wound site of a live adult zebrafish after 23:00 (K), 23:02 (L), 23:06 (M) and 23:18 (N) of time-lapse imaging (h:min). See Movie 1 for the full time-lapse sequences, including the images in C-N. Arrows indicate two neutrophils migrating inside a lymphatic vessel. Scale bars: 1 mm in B-F; 250 µm in G-J; 25 µm in K-N.

Development (2022) 149, dev199667. doi:10.1242/dev.199667

wounding (Fig. 4, Movie 2). Neutrophils began to migrate to the wound in the first 3.5 h (Fig. 4C-E), and large numbers of highly active neutrophils were observed at the wound site at 1 and 2 days post wounding (Fig. 4F-K). By 7 days post-injury the numbers of neutrophils were strongly reduced, to approximately baseline levels and the few neutrophils that remained were quiescent (Movie 2), but we observed overgrowth of Mrc1a-positive lymphatic vessels into the wound area (Fig. 4L-N).

To further validate the broad utility of our intubation system, we also intubated and imaged a 6-month-old Mexican cavefish (*Astyanax mexicanus* – pachón) for 3.5 h (Fig. S6, Movie 3), demonstrating that we can use 405 nm autofluorescence to acquire highly detailed images of bony elements in the face, trunk and scales of the cavefish (Fig. S6C,D,F,H). We also showed that we could clearly image robust blood flow through blood vessels of the intubated animal using transmitted light (Fig. S6E,G, Movie 3).

DISCUSSION

We have developed a new intubation technique that permits long-term and high-resolution imaging of adult zebrafish and cavefish on inverted microscopes, and have provided detailed information, including 3D CAD files for custom 3D-printing an imaging chamber, that will allow other laboratories to easily reproduce our methods. The steadiness and reproducible positioning of the microscope field captured in these high-magnification images (Movies 1-3) shows that animals intubated and mounted for imaging using this method are extremely stable, and that long-term continuous imaging can be performed even at very high optical resolution, followed by fish revival and recovery (Movie 4). Together, our time-lapse images show that this intubation rig is useful both for large field of view imaging (Fig. 3C-J, Movie 1), such as visualizing neutrophil trafficking and migration on a larger scale (Movie 1), as well as for much higher magnification imaging for the visualization and tracking of the precise movements and morphologies of individual cells (Fig. 3K-N, Movie 1).

Using pigment-free *casper* fish was important to this work because, although blood vessels in the scales can be imaged, imaging any structures below the skin becomes very difficult with normally pigmented fish. Researchers using *casper* fish should be aware that there may be physiological differences between *casper* fish and wild-type fish, as has been demonstrated in the hair cells in the lateral line (Holmgren and Sheets, 2021). It is also important to note, once again, that, although we have shown neutrophil recruitment is not appreciably affected by overnight intubation

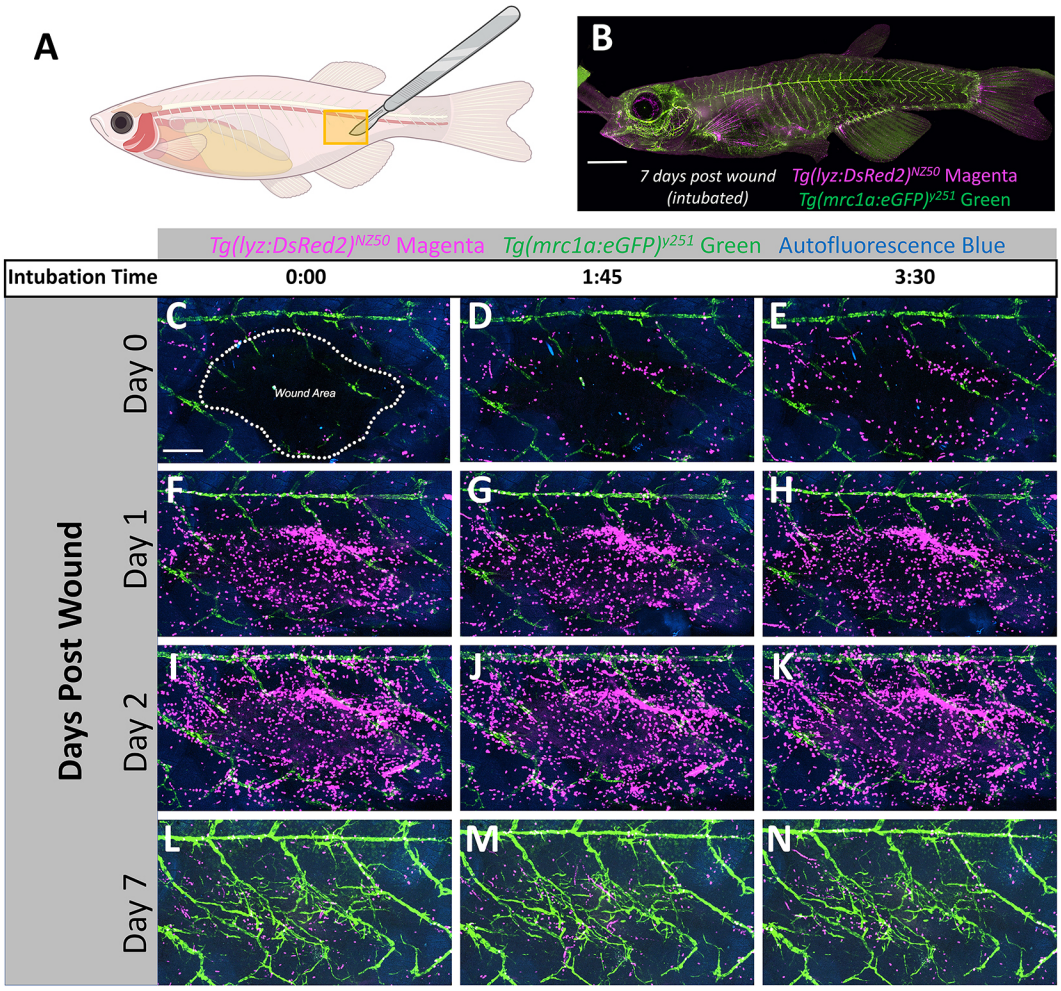

Fig. 4. Repeated intubation and imaging of a small wound. (A) Schematic diagram of an adult *casper* *Tg(lyz:DsRed2)*^{NZ50}*;Tg(mrc1a:eGFP)*^{y251} double transgenic zebrafish. The approximate site of scale removal by abrasion with a scalpel is noted with a yellow box. (B) An overview image of the intubated fish 7 days post-wounding. Fluorescent neutrophils (magenta), lymphatic vessels (green) and auto-fluorescent scales (blue) are visible. (C-N) Confocal images taken at the beginning (0:00), halfway through (1:45) and at the end of a 3.5 h intubation that was repeated four times (on day 0, 1, 2 and 7). Outline of the wound area is indicated by a dotted line in C. Scale bar: 2.5 mm in B; 500 µm in C. See Movie 2 for full time-lapse sequences.

Development (2022) 149, dev199667. doi:10.1242/dev.199667

and imaging, prolonged intubation and imaging may cause other physiological changes within the fish, and appropriate controls must always be included, depending on the process being studied.

This study documents an easy to implement, easy to use, highly effective system for long-term time-lapse imaging of intubated adult zebrafish and cavefish on an inverted microscope. This new system will make it possible to use high-resolution time-lapse optical imaging to study tissue regeneration in the fin, immune responses to injury, cancer metastasis, cellular trafficking through newly described intracranial lymphatic vessels and other important processes taking place in adult zebrafish. In addition to being designed for widely used inverted microscope configurations, the design also incorporates many additional useful new attributes, including precise temperature control, multiple water overflow safety prevention features and an easily replicated and modified 3D printed imaging chamber. The downloadable plans for this imaging chamber can easily be modified and adapted to create chambers to fit any commercial microscope stage. With ever-increasing use of the adult zebrafish as a model for studying disease, regeneration and neurobiology, etc., this imaging 'rig' will become an increasingly vital tool for long-term imaging of key events in adult fish.

MATERIALS AND METHODS

Construction of the intubation and imaging chamber

A 3D printable plastic chamber was designed that would hold a glass-bottomed chambered coverglass, allow inflow and outflow tubing to enter and exit, hold a water sensor and an overflow tube, and fit on our existing Tokei Hit heated microscope stage (model INUB-TIZB; Fig. 1E). A second version of the chamber was also designed to fit on any stage designed to accept a 96-well plate (e.g. Tokei Hit model STZF-TIZWX-SET), with four supporting arms that can be quickly adjusted in CAD software to fit any other microscope stage (Fig. 1F). 3D models for the printable plastic chambers were designed using Google SketchUp Pro, and these CAD designs have been deposited in the NIH 3D Print Exchange under accession number 3DPX-016689. They can be downloaded and used to print the imaging chambers described above. These CAD designs are easily modified to create chambers to fit other microscope stages. Chambers can be printed in-house if 3D printing is available, or there are many 'print and ship' options available. The material used for printing must be watertight and inert. Our chambers were printed out of Nylon 12 by Xometry (xometry.com) using Selective Laser Sintelating (SLS).

A single-well chambered coverglass (Lab-TekII 155360) was placed into the opening in the bottom of the 3D printed chamber by placing a small bead of silicone grease (SG-ONE 24708) around the outer edge of the chambered coverglass using a 12 cc syringe and then pressing it firmly in place (Fig. 2A, Fig. S1). The 3D-printed chamber should be filled with water to test for leaks in the seal before use. Care should be taken to use only enough grease to create a water-tight seal. Excess grease can contaminate the bottom of the coverglass or, worse, onto the objective lens of the microscope.

Water flow

Aquarium system water (1 l) with 126 mg/l tricaine [Tricaine S by Syndel ver. 121718, buffered to pH 7 with 1 M Tris (pH 9)] is placed in a bottle with an air stone inside to aerate the system water. A four-channel peristaltic pump (World Precision Instruments Peri-Star Pro PERIPRO −4 l) is used to pump the aquarium system water through silicone tubing (Tygon), which is wrapped around a heat block (SH100 Mini Dry Bath Hot Block) to warm the water before it goes through the inflow hole in the 3D printed chamber (Fig. 2D). Wrapping the Tygon tubing around the heat block six times and setting the heat block to 57°C produced a water temperature between 24 and 28°C (Fig. S2) inside the chambered coverglass. The tube is held to the bottom of the chambered coverglass using modeling clay (Fig. 2B,C). A small piece of tubing is placed in the end of the outflow tube, small enough to fit in the fish's mouth (Fig. 2C). Setting the peristaltic pump at 15 rotations per min provides a flow rate of 6 ml per min through the chambered coverglass, but flow rate should be measured and adjusted for each rig. Depending on the imaging being carried out, the peristaltic pump creates a pulsatile flow that can cause excessive movement. To prevent pulsatile movement related to the peristaltic pump, a pulse dampener, either commercially available or self-made (Fig. S3), is placed in-line before the heat block. Two outflow tubes are connected to the same peristaltic pump and draw water out of the chambered coverglass and back into the bottle (Fig. 2D). These tubes go through the two specially designed holes in the 3D printed chamber and attach to elbow fittings and another small length of tube (Fig. 2B,C). The height at which these outflow tubes are placed will determine the water level inside the chambered coverglass and should be set so that the fish is completely submerged but the chambered coverglass does not overflow (Fig. 2C). The temperature of the water flowing through the imaging chamber was measured using a digital thermometer (Fisherbrand Traceable thermometer 15-081-111) and maintained between 24 and 28°C by adjusting the temperature of the heat block (Fig. S2). A detailed, step-by-step set up guide for our intubation system is provided in Fig. S1.

Overflow prevention safety features

Overflow of water onto the microscope would be catastrophic, so we developed several features to prevent it. First, there is one small diameter tube (in the fish's mouth) bringing water into the chambered coverglass but two redundant larger diameter tubes removing water so even if one tube becomes clogged the inflow rate will still not exceed the outflow rate. Second, we incorporated an automatic electronic water overflow cut-off switch. We placed a WasherWatcher Laundry Tub Overflow Protector (Overflow Protector) (HydroCheck, STAK Enterprises) into a sensor holder designed into the 3D printed chamber (cut to fit) (Fig. 1B). This product is not always available, so we also modified a Water Watcher Leak Detector Alarm (HydroCheck, STAK Enterprises) with modification details shown in Fig. S4. The Overflow Protector is plugged into an outlet, and the peristaltic pump is plugged into the Overflow Protector. In the event that water overflows the chambered coverglass and enters the 3D printed chamber, the water sensor will detect it and cut the power to the peristaltic pump, preventing additional water entering the chamber. Third, we designed a last-resort emergency overflow outlet from the chamber to prevent water overflowing the chamber if all else fails. A large hole in the upper part of the 3D printed chamber (Fig. 1E,F) accepts a fitting held in place by a greased (silicone grease) 'O' ring attached to a large-diameter tube leading to an empty 1 l bottle (Fig. 1B and Fig. 2B). If the other leak prevention measures fail and water reaches the large overflow hole, water will be drained safely away from the microscope and into the empty bottle.

Fish preparation

Adult *casper* double transgenic zebrafish, *Tg(lyz:DsRed2)*^{NZ50}*;Tg(mrc1a:eGFP)*^{y251} between 6 and 18 months, not fed on the day of the intubation, were anesthetized in 168 mg/l buffered tricaine (note 25% higher than that circulating in the chamber) in system water. A small wound was made around the trunk midline above the anal fin using a 4 mm dissecting knife (Fine Science Tools 10055-12). A few scales were removed by scraping the tip of the knife along the side of the fish from dorsal to ventral; gentle scraping was continued until minor damage to the skin occurred, causing a very small amount of blood to be seen around the wound site. The fish was then placed into the chambered coverglass inside the 3D printed chamber with the wound side facing down. The chamber was placed on the stage of a nearby stereo microscope, then, using two pairs of forceps, one to manipulate the intubation tube (blunt forceps) and one to manipulate the fish (soft tip tweezers, Exceltra 162DRT 18-100-921), the intubation tube was carefully placed into the fish's mouth (Movie 4). Turning off the peristaltic pump is helpful while placing the tube inside the fish's mouth. To prevent movement during image acquisition, a sponge cut to fit inside the chambered coverglass was gently placed on top of the fish (Fig. 2B,C). If additional stabilization for higher magnification imaging is needed, stabilizing weights were used instead of a sponge. Stabilizing weights were made by cutting a finger off of a nitrile glove, filling it with glass beads (425-600 µm Sigma G8772) and tying it off so the beads do not escape. If the fish being intubated needs to be revived after intubation, we found that replacing the tricaine water with system water and letting it run through the

Development (2022) 149, dev199667. doi:10.1242/dev.199667

rig for 10 to 15 min until the fish begins to move was the best way to recover fish.

Fish husbandry and fish strains

Fish were housed in a large zebrafish-dedicated recirculating aquaculture facility (four separate 22,000 l systems) in 6 l and 1.8 l tanks. Fry were fed rotifers and adults were fed Gemma Micro 300 (Skretting) once per day. Water quality parameters were routinely measured and appropriate measures were taken to maintain water quality stability (water quality data available upon request). The following transgenic fish lines were used for this study: *Tg(mrc1a:eGFP)*^{y251} (Jung et al., 2017) and *Tg(lyz:DsRed2)*^{nz50} (Hall et al., 2007). Fish were maintained and imaged in a *casper* [*roy*^{a9} (Ren et al., 2002), *nacre*^{w1} (Lister et al., 1999) double mutant (White et al., 2008)] genetic background in order to increase clarity for visualization by eliminating melanocyte and iridophore cell populations from distorting images. Cavefish were maintained on a recirculating water system with 14/10 h light cycle in groups of 16-20 fish per tank. Adult cavefish were fed Gemma 500 and frozen brine shrimp. This study was performed in an AAALAC accredited facility under an active research project overseen by the NICHD ACUC, Animal Study Proposal 18-015 for zebrafish and 18-016 for cavefish.

Image acquisition

Confocal images of lymphatics and neutrophils were acquired using a Nikon Ti2 inverted microscope with Yokogawa CSU-W1 spinning disk confocal, Hamamatsu Orca Flash 4 v3 camera with the following Nikon objectives: 2× Air 0.1 N.A., 4× Air 0.2 N.A., 10× Air 0.45 N.A. and 20× Air 0.7 N.A. Transmitted light images and movies of cavefish blood flow (Fig. S6E,G and Movie 3) required a very bright transmitted light source to penetrate through the fish; we used the Sola Lumencore Light Engine. Stereo microscope pictures were taken using a Leica M165 microscope with Leica DFC 7000 T camera. In addition to acquiring *Tg(mrc1a:eGFP)*^{y251} expressing lymphatics with a 488 nm excitation laser and *Tg(lyz:DsRed2)*^{NZ50} with a 561 nm laser, we also acquired autofluorescence in the scales using 405 nm excitation laser and used these images to delineate the wound area. Video of the chamber on the inverted microscope and fish swimming stages of Movies 1, 3 and 4 were taken with an iPhone XR. Pictures in Fig. S1 were taken using a Sony α 6400 mirrorless camera.

Image processing and statistics

Images were processed using Nikon Elements. Maximum intensity projections of confocal stacks are shown. Time-lapse movies were made using Nikon Elements and exported to Adobe Premiere Pro CC 2019. Adobe Premiere Pro CC 2019 and Adobe Photoshop CC 2019 were used to add labels and arrows to movies. Schematics were made using Adobe Photoshop CC 2019, Microsoft PowerPoint and BioRender software.

Neutrophil coverage area (Fig. 4) was measured on maximum intensity projections of 2× tiled confocal stacks using Nikon Elements General Analysis 3 software. Regions of interest of the same area were selected, and calculated at the start and end of the intubation session using the same threshold. The change in control area was calculated by subtracting the neutrophil area coverage at the beginning of intubation from coverage at the end of the intubation. Because the wound area had fewer neutrophils than the control area, we subtracted the wound area at the end of intubation from the control area at the beginning of intubation to prevent an over-estimation of change in neutrophil coverage area.

We compared the mean change in neutrophil coverage areas of the wound to the control areas using a two-tailed *t*-test assuming unequal variances, and used the Holm-Bonferroni method to counteract the problem of multiple tests (Holm, 1979). We used GraphPad Prism 9 and Microsoft Excel to compile data, run statistics and create the plot (Fig. S5K).

Intubation system maintenance

After each use, the intubation system should be cleaned by running a 1:10 bleach solution through the system for at least 10 min followed by at least two flushes of tap water to remove any residual bleach. The tube sections that are used in the peristaltic pump become worn out quickly and should be replaced between uses. All of the tubing needs to be replaced occasionally, especially if any mold, mildew or bacterial growth is seen. The chambered coverglass can be cleaned with 70% ethanol between uses but also needs to be replaced when it can no longer be effectively cleaned.

Acknowledgements

The authors thank members of the Weinstein laboratory for their critical comments on this manuscript. The authors also thank the Research Animal Branch of the Eunice Kennedy Shriver National Institute of Child Health and Human Development as well as the Charles River staff for excellent animal care and husbandry.

Competing interests

The authors declare no competing or financial interests.

Author contributions

Conceptualization: D.C., B.S., M.V.G., A.V.G., B.M.W.; Methodology: D.C., B.S., M.V.G., A.V.G., B.M.W.; Validation: D.C., B.S.; Formal analysis: D.C., B.S.; Investigation: D.C., A.E.G., J.S.P., B.M.W.; Resources: A.E.G., B.M.W.; Data curation: D.C.; Writing - original draft: D.C., B.S., B.M.W.; Writing - review & editing: D.C., M.V., B.M.W.; Visualization: D.C., J.S.P., B.M.W.; Supervision: D.C., B.M.W.; Project administration: B.M.W.; Funding acquisition: B.M.W.

Funding

This work was supported by the intramural program of the Eunice Kennedy Shriver National Institute of Child Health and Human Development, National Institutes of Health (ZIA-HD008915, ZIA-HD008808 and ZIA-HD001011 to B.M.W.). Deposited in PMC for release after 12 months.

Peer review history

The peer review history is available online at https://journals.biologists.com/dev/article-lookup/doi/10.1242/dev.199667.

References

Castranova, D., Samasa, B., Venero Galanternik, M., Jung, H. M., Pham, V. N. and Weinstein, B. M. (2021). Live imaging of intracranial lymphatics in the zebrafish. *Circ. Res.* **128**, 42-58. doi:10.1161/CIRCRESAHA.120.317372

Cox, B. D., De Simone, A., Tornini, V. A., Singh, S. P., Di Talia, S. and Poss, K. D. (2018). In toto imaging of dynamic osteoblast behaviors in regenerating skeletal bone. *Curr. Biol.* **28**, 3937-3947.

Driever, W., Solnica-Krezel, L., Schier, A. F., Neuhauss, S. C., Malicki, J., Stemple, D. L., Stainier, D. Y., Zwartkruis, F., Abdelilah, S., Rangini, Z. et al. (1996). A genetic screen for mutations affecting embryogenesis in zebrafish. *Development* **123**, 37-46. doi:10.1242/dev.123.1.37

Fazio, M., Ablain, J., Chuan, Y., Langenau, D. M. and Zon, L. I. (2020). Zebrafish patient avatars in cancer biology and precision cancer therapy. *Nat. Rev. Cancer* **20**, 263-273. doi:10.1038/s41568-020-0252-3

Frantz, W. T. and Ceol, C. J. (2020). From tank to treatment: modeling melanoma in zebrafish. *Cells* **9**. 1289. doi:10.3390/cells9051289

Hall, C., Flores, M. V., Storm, T., Crosier, K. and Crosier, P. (2007). The zebrafish lysozyme C promoter drives myeloid-specific expression in transgenic fish. *BMC Dev. Biol.* **7**, 42. doi:10.1186/1471-213X-7-42

Holm, S. (1979). A simple sequentially rejective multiple test procedure. *Scand J Stat* **6**, 65-70.

Holmgren, M. and Sheets, L. (2021). Influence of Mpv17 on hair-cell mitochondrial homeostasis, synapse integrity, and vulnerability to damage in the zebrafish lateral line. *Front Cell Neurosci* **15**, 693375. doi:10.3389/fncel.2021.693375

Hwang, W. Y., Fu, Y., Reyon, D., Maeder, M. L., Tsai, S. Q., Sander, J. D., Peterson, R. T., Yeh, J.-R. and Joung, J. K. (2013). Efficient genome editing in zebrafish using a CRISPR-Cas system. *Nat. Biotechnol.* **31**, 227-229. doi:10.1038/nbt.2501

Johnson, S. L. and Weston, J. A. (1995). Temperature-sensitive mutations that cause stage-specific defects in Zebrafish fin regeneration. *Genetics* **141**, 1583-1595. doi:10.1093/genetics/141.4.1583

Jung, H. M., Castranova, D., Swift, M. R., Pham, V. N., Venero Galanternik, M., Isogai, S., Butler, M. G., Mulligan, T. S. and Weinstein, B. M. (2017). Development of the larval lymphatic system in zebrafish. *Development* **144**, 2070-2081.

Kamei, M. and Weinstein, B. M. (2005). Long-term time-lapse fluorescence imaging of developing zebrafish. *Zebrafish* **2**, 113-123. doi:10.1089/zeb.2005.2.113

Kaufman, C. K., Mosimann, C., Fan, Z. P., Yang, S., Thomas, A. J., Ablain, J., Tan, J. L., Fogley, R. D., van Rooijen, E., Hagedorn, E. J. et al. (2016). A zebrafish melanoma model reveals emergence of neural crest identity during melanoma initiation. *Science* **351**, aad2197.

Lawson, N. D. and Weinstein, B. M. (2002). In vivo imaging of embryonic vascular development using transgenic zebrafish. *Dev. Biol.* **248**, 307-318. doi:10.1006/dbio.2002.0711

Lister, J. A., Robertson, C. P., Lepage, T., Johnson, S. L. and Raible, D. W. (1999). nacre encodes a zebrafish microphthalmia-related protein that regulates

neural-crest-derived pigment cell fate. *Development* **126**, 3757-3767. doi:10.1242/dev.126.17.3757

Mullins, M. C., Hammerschmidt, M., Haffter, P. and Nüsslein-Volhard, C. (1994). Large-scale mutagenesis in the zebrafish: in search of genes controlling development in a vertebrate. *Curr. Biol.* **4**, 189-202. doi:10.1016/S0960-9822(00)00048-8

Nasevicius, A. and Ekker, S. C. (2000). Effective targeted gene 'knockdown' in zebrafish. *Nat. Genet.* **26**, 216-220. doi:10.1038/79951

Ober, E. A., Field, H. A. and Stainier, D. Y. (2003). From endoderm formation to liver and pancreas development in zebrafish. *Mech. Dev.* **120**, 5-18. doi:10.1016/S0925-4773(02)00327-1

Oka, T., Nishimura, Y., Zang, L., Hirano, M., Shimada, Y., Wang, Z., Umemoto, N., Kuroyanagi, J., Nishimura, N. and Tanaka, T. (2010). Diet-induced obesity in zebrafish shares common pathophysiological pathways with mammalian obesity. *BMC Physiol.* **10**, 21. doi:10.1186/1472-6793-10-21

Patton, E. E. and Zon, L. I. (2001). The art and design of genetic screens: zebrafish. *Nat. Rev. Genet.* **2**, 956-966. doi:10.1038/35103567

Poss, K. D., Wilson, L. G. and Keating, M. T. (2002). Heart regeneration in zebrafish. *Science* **298**, 2188-2190. doi:10.1126/science.1077857

Ren, J. Q., McCarthy, W. R., Zhang, H., Adolph, A. R. and Li, L. (2002). Behavioral visual responses of wild-type and hypopigmented zebrafish. *Vision Res.* **42**, 293-299. doi:10.1016/S0042-6989(01)00284-X

Scheer, N. and Campos-Ortega, J. A. (1999). Use of the Gal4-UAS technique for targeted gene expression in the zebrafish. *Mech. Dev.* **80**, 153-158. doi:10.1016/S0925-4773(98)00209-3

White, R. M., Sessa, A., Burke, C., Bowman, T., LeBlanc, J., Ceol, C., Bourque, C., Dovey, M., Goessling, W., Burns, C. E. et al. (2008). Transparent adult zebrafish as a tool for in vivo transplantation analysis. *Cell Stem Cell* **2**, 183-189. doi:10.1016/j.stem.2007.11.002

Wyart, C. and Del Bene, F. (2011). Let there be light: zebrafish neurobiology and the optogenetic revolution. *Rev. Neurosci.* **22**, 121-130. doi:10.1515/rns.2011.013

Wyart, C., Del Bene, F., Warp, E., Scott, E. K., Trauner, D., Baier, H. and Isacoff, E. Y. (2009). Optogenetic dissection of a behavioural module in the vertebrate spinal cord. *Nature* **461**, 407-410.

Xu, C., Volkery, S. and Siekmann, A. F. (2015). Intubation-based anesthesia for long-term time-lapse imaging of adult zebrafish. *Nat. Protoc.* **10**, 2064-2073. doi:10.1038/nprot.2015.130

Yan, C., Brunson, D. C., Tang, Q., Do, D., Iftimia, N. A., Moore, J. C., Hayes, M. N., Welker, A. M., Garcia, E. G., Dubash, T. D. et al. (2019). Visualizing Engrafted Human Cancer and Therapy Responses in Immunodeficient Zebrafish. *Cell* **177**, 1903-1914.

Yaniv, K., Isogai, S., Castranova, D., Dye, L., Hitomi, J. and Weinstein, B. M. (2006). Live imaging of lymphatic development in the zebrafish. *Nat. Med.* **12**, 711-716. doi:10.1038/nm1427